Electronic properties of armchair & zigzag single-walled carbon nanotubes

Rana Hamood (1)
Zina A. Al Shadidi (2,*)
Samia Jamal (3)

Received: 13/01/2024
Revised: 09/03/2024
Accepted: 30/05/2024

---

[1] Department of Physics, Saber Faculty of science and Education, University of Lahej, Yemen. Email: rana.hammoud.edu.s@aden-univ.net
[2] Department of Radiology, Al Ma'moun University College, Baghdad/ Iraq. Email: zabaqer@yahoo.com
[3] Department of Physics, Saber Faculty of science and Education, University of Lahej, Yemen. Email: xenaabdulameer@gmail.com
* Corresponding Author Designation, Email: zabaqer@yahoo.com

https://doi.org/10.20428/jst.v29i1.2256

Electronic properties of armchair & zigzag single-walled carbon nanotubes

Rana Hamood
Department of Physics, Saber Faculty of science and Education, University of Lahej, Yemen.
rana.hammoud.edu.s@aden-univ.net

Zina A. Al Shadidi
Department of Radiology, Al Ma'moun University College.
Baghdad - Iraq.
zabaqer@yahoo.com

Samia Jamal
Department of Physics, Saber Faculty of science and Education, University of Lahej, Yemen.
xenaabdulameer@gmail.com

Abstract_ ***The purpose of this work is to examine the influence of chirality on the electronic band structure in armchair and zigzag single-walled carbon nanotubes (SWCNTs). The tight-binding model has been used to simulate electrical band gaps for single-walled carbon nanotubes (SWCNTs) with different chiral indices. The total number of bands in the electronic band structure increases as chirality increases. A study was conducted on the band gap at Fermi energy (E=0) and it was found that the electronic band structure in armchair and zigzag (SWCNTs) can be either metallic or semiconductor depending on chirality. Additionally supplied are the tube's diameter and the band gap value. The impact of changes in the oxide thickness and CNT channel length on the gate capacitance and drain current have been analyzed. The findings validate showed good agreement with the experimental and theoretical results.***

Keywords— *Single walled Carbon nanotubes, electronic band structure, tight binding model, Carbon nanotube field effect transistor.*

I. INTRODUCTION

In the electronic band, carbon nanotubes) CNTs), have garnered a lot of interest. Since these tubes were created by several groups [1-3]. The chirality (n, m) represents the wrapping of the graphite sheet and is a crucial characteristic to take into account while building a carbon nanotube. It needs to be further studied because of its role in a CNT's structure [4]. A single-walled carbon nanotube (SWCNT) can be classified as an armchair structure when the values of n, m, and l are equal, where l is an integer. On the other hand, a zigzag SWCNT is formed when n is equal to l and m is equal to 0, while every other combination of n and m results in the formation of a chiral carbon nanotube [5,6]. Together with other many characteristics, the electrical properties of SWCNTs can directly alter their geometrical structure. By diffraction of quantum mechanical electron waves along the Bravais lattice, the band structure of a specific periodic crystal lattice is derived. Band structure affects a variety of material properties, including optical, electrical, and others [1]. According to the previous research for electronic band structure computations [7, 8], the metallic and semiconducting behavior of (SWCNTs) can be predicted by the (n,m) indices. In the case of n - m $\neq$3l, the SWCNTs will be semiconducting with energy gaps of~0.5 eV [9]. Therefore, if n $\neq$ 3 l (where l is an integer), the armchair (n, n) SWCNTs are projected to be metallic, and the zigzag (n, 0) SWCNTs to be semiconducting. The diameter of the nanotube decides the semiconducting energy gap in the (SWCNTs) [10].

Later, nanotubes of other inorganic substances such as silicon nanotubes [11], MoS2 nanotubes [12] and GaSe nanotubes [13] have been observed and successfully synthesized. Single carbon nanotubes have a maximum current density of 1013 A/m2, which is noticeably higher than that of most metals and semiconductors Nanotubes also have the property of being inert and having no surface states, which makes them extremely compatible with other materials, including oxides. Compared to other molecular devices, carbon nanotubes are more desirable because of these qualities. The goal of state-of-the-art research is to minimize feature sizes in semiconductor technology by using the unique features of carbon nanotubes to create a variety of devices [14]. A carbon nanotube field effect transistor (CNTFET) is a type of transistor that employs either a single carbon nanotube or an array of carbon nanotubes as the channel material, rather than the traditional use of bulk silicon in the construction of a MOSFET [15].

This paper presents the energy gaps for each type of carbon nanotube. Simulations of the current-voltage characteristics as functions of factors like the gate thickness and CNTFET length are investigated. Additionally, I-V characteristics of the CNTFET are also examined.

II. COMPUTATIONAL METHODOLOGY

One effective tool for studying carbon nanotubes is computer simulation. Through simulations, the characteristics of carbon nanotubes with any chirality can be predicted. A popular and widely applied method for simulating single-wall carbon nanotubes electronic structure is the Tight Binding (TBM) Method [16].

A. Tight Binding (TBM) Method:

This technique is well-known in the field of solid-state physics and works effectively in situations when the atomic wave functions in an insulating crystal have a weak overlap. For comprehending the basic properties of band structure in single-walled carbon nanotubes, TBM is the most suitable method [16, 8]. This method makes a linear combination of atomic orbitals, which are locations for the different atoms in the crystal. This idea was first by the Bloch Tight Binding Approximation (TBA. Bloch theorem is applicable which can be written as) [17]:

$$T\psi_k(r) = e^{ik.a_i}\psi_k(r) \qquad \textbf{(1)}$$

Where k is the vector of the Bloch wave and T is the translational operator in the direction of a_i. Generally, in the tight-binding model, the atomic orbitals are used to express single electron wave functions.

The wave function $\phi j\ (k, r)$ on site j can be defined as a summation of the atomic wave functions $(r -)$.

$$\phi_j(k,r) = \frac{1}{\sqrt{N}} \sum_{R_j}^{N} e^{ik.R_j}\, \varphi(r - R_j) \qquad \textbf{(2)}$$

Where N is the number of atomic wave functions in the unit cell and Rj is the location of the jth atom. These Bloch functions can be combined linearly to form flows, which are the eigen functions in a crystal:

$$\psi_j(k,r) = \sum_{j'=1}^{n} c_{jj'}\,(k)\phi_j(k,r) \qquad \textbf{(3)}$$

Where c_{jj}, (k) are yet to be determined coefficients. The Schrodinger equation quantum mechanically has been solved mechanically to get the dispersion relation of the crystal, as follows:

$$H\psi_k = E(K)\psi_k \qquad \textbf{(4)}$$

The eigenvalues E(k) will be the energy bands of the crystal.

B. Electronic Band Structure of SWCNTs:

The band structure of carbon nanotubes (CNTs) can be derived from the band structure of graphene. To proceed, let us start by deriving the two-dimensional (2D) electronic band structure of graphene, which can be represented as [9].

$$[E(\vec{k})] = \pm t\sqrt{1 + 4\cos\left[k_x\left(3\frac{a_{cc}}{2}\right)\right]\cos\left[k_x\left(\sqrt{3}\frac{a_{cc}}{2}\right)\right] + 4\cos^2\left[k_x\left(\sqrt{3}\frac{a_{cc}}{2}\right)\right]} \qquad \textbf{(5)}$$

where, t = 2.6eV is the hopping parameter, acc = 1.42 × 10−10m is the c-c bonding distance, and the (+) and (−) signs symbolizes the conduction and valence bands respectively. Quantizing the wave vector in the circumferential direction yields the structure of the electronic band of carbon nanotubes from graphene. If CNT can be considered as an infinitely long cylinder, there are two wave vectors associated with it: (1) the wave vector parallel to CNT axis k|| that is continuous in nature due to the infinitely long length of CNTs and (2) the perpendicular wave vector k⊥ that is along the circumference of CNT. These two wave vectors must satisfy a periodic boundary condition.

$$\vec{K}_\perp \cdot \vec{C_h} = \pi d_{(SWCNT)}\ \vec{K}_\perp = 2\pi\upsilon \qquad \textbf{(6)}$$

Where ***d*** (SWCNT) is the diameter of a SWCNT and υ is an integer.

As a result, each band of graphene splits into a number of 1-D sub-bands labeled by p. The quantized values of allowed k⊥ for SWCNTs are a result of this boundary condition. By cross-sectionally cutting the band structure of 2D graphene with these allowed k⊥ states, the 1D band structure of SWCNTs can be obtained. This is called zone- folding scheme of obtaining the band structure [9, 18].

1) Electronic Band Structure of Armchair SWCNT:

Chirality (n, m) for an Armchair SWCNT is defined in the following manner: n=m and n, m are integers. CNTs are named after the pattern that appears on the edge of the circumference, thus, it can be inferred that the Armchair CNT is so-named based on the pattern that appears along the edge of its chiral vector. Figure (1) illustrates that the x-direction is represented by the circumference of the SWCNT, while the tube axis is parallel to the y-direction [19].

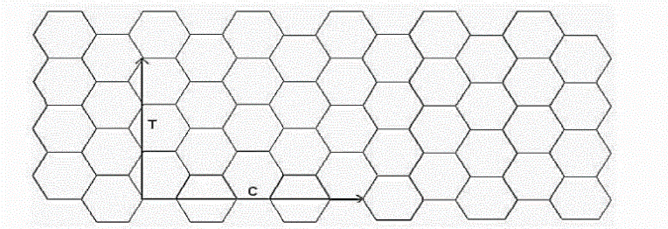

Figure (1): Chiral and transport vectors of Armchair CNT

The circumference of SWCNT is given by [19]:

$$\vec{C_h} = \sqrt{3}a_{c-c}\sqrt{n^2 + m^2 + nm} \qquad (7)$$

Since Armchair must be n=m, the circumference of Armchair SWCNT in x-direction is:

$$\vec{C_h} = 3na_{c-c}\hat{x} \qquad (8)$$

https://doi.org/10.20428/jst.v29i1.2256

Therefore, the periodic boundary condition equation (6) becomes:

$$\vec{\mathrm{K}}_{\mathrm{x}} \cdot \vec{\mathrm{C}_{\mathrm{x}}} = 2\pi\upsilon \tag{9}$$

$$\vec{\mathrm{K}}_{\mathrm{x}} \cdot 3\mathrm{na}_{\mathrm{cc}} = 2\pi\upsilon \tag{10}$$

$$\vec{\mathrm{K}}_{\mathrm{x}} = \frac{2\pi\upsilon}{3\mathrm{na}_{\mathrm{cc}}} \tag{11}$$

Upon substituting the values of υ and n in equation (11), the ky-axis is parallel to the acceptable values of K ⃗_x. Thus, the quantized circumferential wave vector K ⃗_x lines passing through the Fermi locations of graphene,, consequently indicating that the Armchair SWCNT lacks a band gap and exhibits metallic properties [18].

Again, by putting the values of kx from equation (11) to equation (5), the Armchair SWCNTs of 1D band structure can be computed as [18]:

$$[\mathrm{E}(\vec{\mathrm{k}})] = \pm t\sqrt{1 + 4\cos\left[\left(\frac{\pi\upsilon}{n}\right)\right]\cos\left[k_t\left(\sqrt{3}\,\frac{a_{cc}}{2}\right)\right] + 4cos^2\left[k_t\left(\sqrt{3}\,\frac{a_{cc}}{2}\right)\right]} \tag{12}$$

2) Electronic Band Structure of zigzag SWCNT

A Zigzag SWCNTs has chirality (n, m) = (n, 0) where n is an integer. As expected, the Zigzag CNT has a Zigzag pattern along its circumferential edge. As illustrated in figure (2), the SWCNT's tube axis is parallel to the x-direction, while the circumference depicts the y-direction[19].

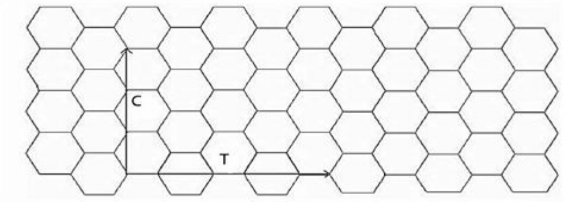

Figure (2): chiral and transport of Zigzag CNT.

In Zigzag SWCNT must be n= integer and m= 0, so equation (7) becomes as follows:

$$\boldsymbol{\overrightarrow{C_h} = \sqrt{3}na_{c-c}\hat{y}} \tag{13}$$

The above Equation represents the circumference of Zigzag SWCNT. Therefore, the periodic boundary condition in Equation (6), becomes as

$$\boldsymbol{\vec{K}_y \cdot \overrightarrow{C_y} = 2\pi\upsilon} \tag{14}$$

$$\boldsymbol{\vec{K}_y \cdot \sqrt{3}na_{c-c} = 2\pi\upsilon} \tag{15}$$

$$\boldsymbol{\vec{K}_y = \frac{2\pi\upsilon}{\sqrt{3}na_{c-c}}} \tag{16}$$

When the quantized circumferential wave vector ky lines make contact with the graphene Fermi sites, this demonstrating the metallic band gap-free nature of the Zigzag SWCNT. But if ky does not intersect the graphene Fermi sites in any other case, this indicating that the Zigzag SWCNT is a semiconductor because it possesses a band gap. [18].

Equation (5) can be used to compute the 1D band of structure Zigzag b applying the values of ky from equation (16) [18, 20]:

$$\boldsymbol{[E(\vec{k})] = \pm t\sqrt{1 + 4\,cos\left[\left(k_t\left(3\,\frac{a_{c-c}}{2}\right)\right)\right]cos\left[\left(\frac{\pi\upsilon}{n}\right)\right] + 4cos^2\left[\left(\frac{\pi\upsilon}{n}\right)\right]}} \tag{17}$$

C. Drain current-voltage characteristics of planar CNTFET

There are two distinct zones on the current-voltage curve: linear and saturation. The drain current in the CNTFET's linear section can be found in the manner described below [21]:

$$\boldsymbol{I_d = \frac{W}{L}\mu C_{ox}\left[(V_{gs} - V_{\mathrm{T}})V_{ds} - \frac{V_{ds}^2}{2}\right]} \tag{18}$$

Where the width of CNTFET is denoted as W, while the length of CNTFET is represented by L, the mobility of carriers is symbolized as μ, and the gate capacitance is referred to as C_{ox}.

III. RESULTS AND DISCUSSION

In the case of CNTs, IF there is a significant quantity of atoms within the system. The merging of higher energy levels results in the formation of two distinct bands of allowable energies, namely the valence band and the conduction band. The band gap, which is sometimes called the energy gap, acts as a separator between the valence and conduction bands' closely spaced energy levels. At EF = 0, the Fermi energy level divides the valence and conduction bands. Analyzing the dispersion relations near the Fermi energy EF = 0 aids in comprehending electrical conduction, as it is impacted by the states surrounding this energy level [22].

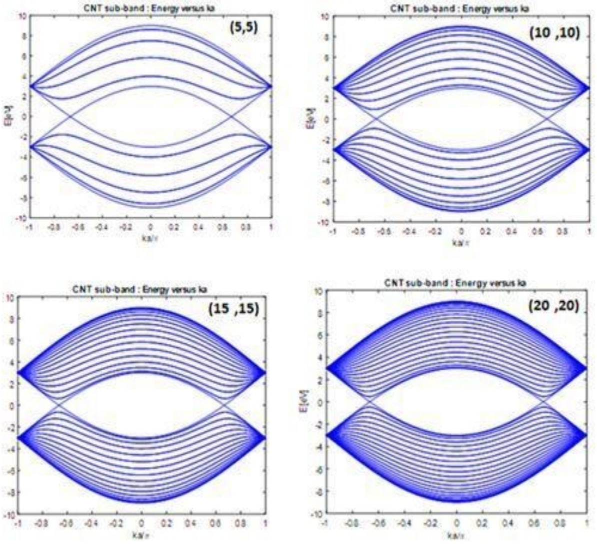

Figure (3). Electronic band structures of Armchair CNT for 5, 10, 15and 20 chirality values.

A. The effect of chirality of armchair and zigzag SWCNTs

Generally, 2n conduction and 2n valence bands on (n,n) Armchair carbon nanotubes give

4n energy sub-bands. Out of these 2n bands, two are non-degenerate and n-1are doubly degenerate. The two sub-bands equal energy dispersions are the cause of the degeneracy. All armchair carbon nanotubes have band degeneracy between the highest valence and the lowest conduction band [22].

The armchair single-walled carbon nanotubes (SWCNTs) with chiralities n = m = 5, 10, 15, and 20 have been analyzed for their electronic band structures, as depicted in figure (3). The findings show that the total number of bands in the armchair SWCNTs' electronic band configurations grows by 4 when their chirality is increased by 1. This discovery implies that the current capability of armchair SWCNTs increases with an increase in carrier count. Notably, the top valence band and lower conduction band of each armchair SWCNT electronic band structure intersect at the Fermi energy (E = 0). As a result, every armchair SWCNT displays metallic characteristics.

The simulation results are agrees with the theoretical results by putting chirality (n=m = integer) value in the equation [9]:

$$N_{band}=\frac{4(n^2+m^2+nm)}{gcd\,(2n+m, 2m+n)} \qquad \textbf{\textit{(19)}}$$

Where N_{band} is the total number of bands in each band structure, gcd stand for greatest common divisor.

For chiralities n= m= 5, 10, 15 and 20, the total number of bands for these chirality values = 20, 40, 60 and 80. For each Armchair chirality values, the equation n – m = 0 which a valid conduction for a metallic SWCNTs. It means all Armchair SWCNTs shows metallic behavior.

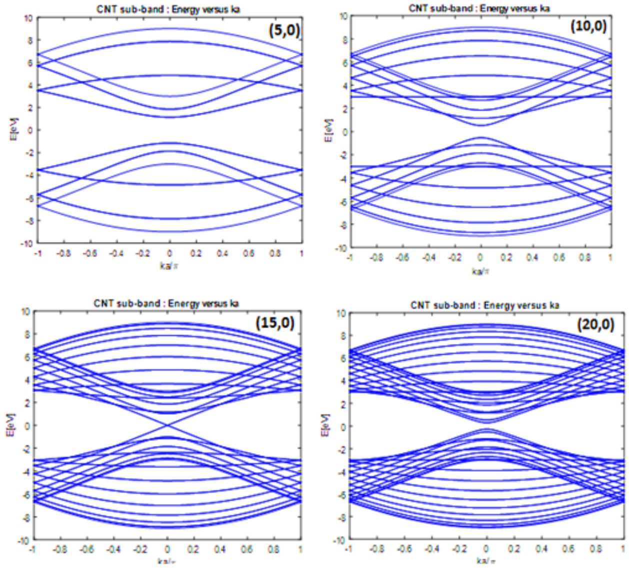

Figure (4): Electronic band structures of Zigzag CNT for 5, 10, 15, 20 chirality values.

Figure (4) illustrates the simulated electronic band structures of Zigzag CNTs with chirality n = 5, 10, 15, and 20. These structures exhibit variations compared to the band structure of Armchair SWCNT, nevertheless the number of bands in the electronic band structures of Zigzag CNTs remains consistent with that of Armchair electronic band structures. The number of bands in the Zigzag CNTs' electrical band structure rises by 4 for every unit increase in chirality value n. The electronic band structure of Zigzag SWCNTs (15, 0) exhibits metallic behavior at the Fermi energy (E = 0), where the upper valance band and lower conduction band intersect. On the other hand, at chirality values of 5, 0, 10, 0, and 20, 0 for Zigzag SWCNTs, a gap separates the lower conduction band from the top valance. Stated differently, at Fermi energy (E = 0), there is no intersection between the upper valance and lower conduction band. The semiconducting behavior is demonstrated by this phenomenon. This occurrence arises from the fact that zigzag tubes transform into a metallic state when the equation n – m = 3 υ is satisfied, where υ represents an integer. If this equation is not met, the tube will continue to exhibit semiconducting properties [22].

In comparison the simulation results with the theoretical results by putting the chirality value (n =integer, m= 0) in equation (19). For values n = 5, 10, 15, and 20, the total number of bands for these chirality values = 20, 40, 60 and 80. Mathematically, the increase in chirality in Zigzag SWCNTs by 1 increase the electronic band structures of Zigzag SWCNT by a factor of 4, resulting in a total number of bands. These results are agreed with the results in [18].

https://doi.org/10.20428/jst.v29i1.2256

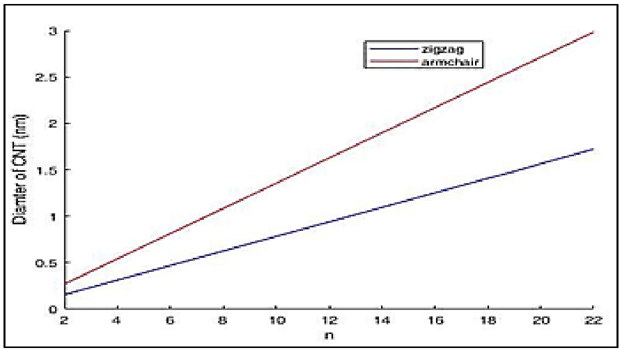

Figure (5): Plot of diameter versus Index (n) for Armchair and Zigzag SWCNTs.

B. Bandgap dependence on diameter for semiconducting Zigzag SWCNTs

Before processing how bandgap varies with diameter, it proves beneficial to know how the diameter varies with index.

The magnitude of the chiral vector that depends on indices (n, m) of CNTs is the circumference of the nanotube. Therefore, when the indices of CNTs increase the circumference of CNTs increases, since the diameter is directly proportional to circumference by a factor($1/\pi$, it is evident that the diameter increases as the indices are increased. Moreover, increasing the index for Armchair and Zigzag SWCNTs leads to increases in their circumference and thus their diameter linearly as depicted in Figure (5). The outcomes are in accordance with the findings of [23].

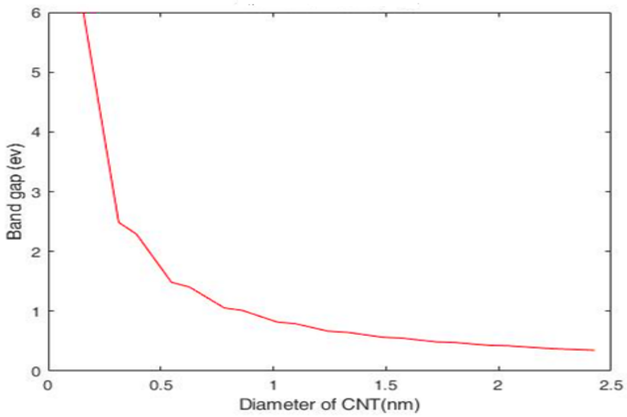

Figure (6): Plot of diameters vs. band gaps of Zigzag SWCNTs.

Figure (6) shows how Zigzag CNTs' bandgap and diameter relate to one another. It is evident that the band gap and diameter have an inverse relationship. Since the diameter of semiconducting Zigzag SWCNTs is directly correlated with chirality, the band gap of these materials is inversely correlated with chirality. When the chirality of the semiconducting Zigzag SWCNTs grows, the band gap between the lower conduction band and higher valance band gets smaller. This further implies that the semiconducting Zigzag SWCNTs' current capacity is increased because less energy is required to move electrons from the valance band to the conduction band [18]. Similarly, Table (1) presents a good agreement with the values of the results by comparing the simulated and experimental band gap of zigzag SWCNT [24].

Table (1): Band gaps of various Zigzag CNTs are compared with respect to diameter.

(n,m)	**Diameter (nm)**	**Simulated Gap (ev)**	**Calculated Gap (ev)**
(1,0)	0.07830	6.000	10.8812
(2,0)	0.15660	6.000	5.44061
(4,0)	0.31315	2.486	2.72074
(5,0)	0.39144	2.292	2.17657
(7,0)	0.54802	1.4818	1.55468
(8,0)	0.62631	1.4082	1.36034
(10,0)	0.78289	1.0542	1.08827
(11,0)	0.86118	1.0156	0.98934
(13,0)	1.01780	0.8178	0.83709
(14,0)	1.09600	0.7934	0.77737
(16,0)	1.25260	0.6668	0.68018
(17,0)	1.33090	0.6462	0.64016
(19,0)	1.48750	0.5634	0.57277
(20,0)	1.56580	0.5522	0.54413
(22,0)	1.72240	0.4876	0.49465
(23,0)	1.80060	0.4792	0.47317
(25,0)	1.95720	0.4299	0.43531
(26,0)	2.03580	0.4237	0.41850
(28,0)	2.19210	0.3844	0.38866
(29,0)	2.27070	0.3700	0.37521
(31,0)	2.42690	0.3476	0.35106

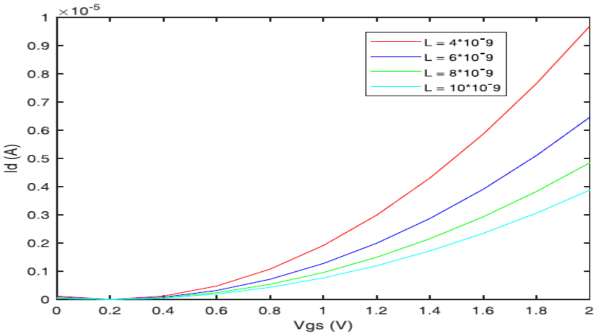

Figure (7): In SWCNTS, drain current versus voltage at various channel lengths.

Figure (7) illustrates the change of drain current (Id) w.r.t gate-source voltage (Vgs) of a single wall CNTFET for different channel lengths. It is shown that the drain current of the CNTFET increases with the shortening of the SWCNT channel length. When the length of the SWCNT channel exceeds several micrometers, the carriers experience scattering during the transportation process, leading to a decrease in carrier mobility [25].

Consequently, the carriers in the SWCNT will perform a ballistic transport if the CNT channel is reduced. As a result, the constructed CNTFET will be successfully enhanced and the device's mobility will be substantially raised.

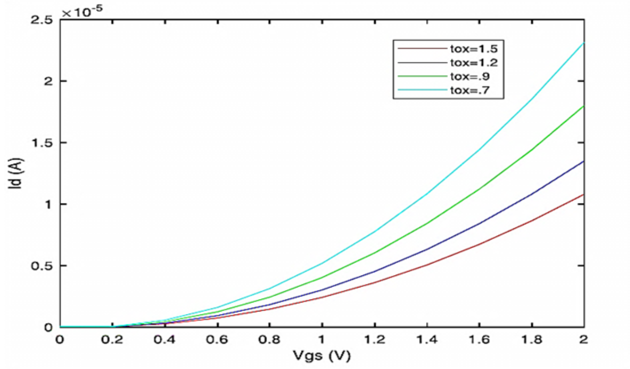

Figure (8): Current at the drain vs gate voltage, and oxide thickness in CNTs.

Figure (8) depicts the relationship between drain-source current (Id) and gate-source voltage (Vgs) for different gate insulator thicknesses in CNTFET. According to observations, the drain current of the CNTFET experiences an increase as the thickness of the gate insulator decreases. This implies that the current capacity improves when the gate insulator thickness is reduced. These results indicate that there is an inverse correlation between the thickness of the gate insulator and the conductivity of the CNTFET [26].

IV. CONCLUSION

The electronic band structures of single-walled carbon nanotubes (SWCNTs) are discussed in this study along with the impact of a change in carbon nanotube diameter on the band structure and an explanation of how SWCNTs behave in terms of being metallic or semiconductor depending on their chirality. The analysis has confirmed that there is an increase of 4 sub-bands with a 1-unit chirality increase in the electronic band structure of both armchair and zigzag single-walled CNTs. The fact that all armchair SWCNTs exhibit metallic behavior, indicating a non-zero band gap, has been further confirmed analytically and through simulations; in contrast, zigzag SWCNTs exhibit both metallic and semiconducting activity. Additionally, it was discovered that while diameter grows with chirality, band gap reduces with diameter. According to the I-V characteristic data, drain current increases when the SWCNT channel length shortens and falls when the oxide thickness in CNTs increases, allowing the carriers to perform a ballistic transit inside the SWCNT. As a result, the device's mobility will be significantly enhanced.

V. FUTURE WORK

Perhaps SWCNTs will be components of future computers used to design new materials with even more remarkable properties. Other SWCNTs configurations such as chiral need also to be studied to more fully understand the effect of interwall interaction on the electronic structure of all SWCNTs

VI. REFERENCES

[1] H. Dai, “Carbon nanotubes: opportunities and challenges,” *Surface Science*, vol. 500, no. 1, pp. 218–241, Mar. 2002, doi: https://doi.org/10.1016/S0039-6028(01)01558-8.

[2] R. J. Chen et al., “Noncovalent functionalization of carbon nanotubes for highly specific electronic biosensors,” *Proceedings of the National Academy of Sciences of the United States of America*, vol. 100, no. 9, pp. 4984–4989, Apr. 2003, doi: https://doi.org/10.1073/pnas.0837064100.

[3] D.S. Bethune, C.H. Kiang, M.S. Devries, G. Gorman, R. Savoy, J. Vazquez, and R. Beyers, “Cobalt-catalyzed growth of carbon nanotubes with single-atomic-layer walls”, *Nature,* vol. 363, (1993) 605-607.

[4] D. Dass, R. Prasher, and R. Vaid, “Analytical study of unit cell and molecular structures of single walled carbon nanotubes”, *International Journal of Computational*, 2012.

[5] M.S. Dresselhaus, G. Dresselhaus, and R. Saito, “Physics of carbon nanotubes”, *Carbon*, vol. 33, (1995) 883-891.

[6] H. R. Tabar, “Computational physics of carbon nanotubes”, Cambridge University Press, New York, 2008.

[7] J. W. Mintmire, B. I. Dunlap, and C. T. White, “Are fullerene tubules metallic?” *Physical Review Letters*, vol. 68, no. 5, (1992) 631–634.

[8] R. Saito, M. Fujita, G. Dresselhaus, and M. S. Dresselhaus, “Electronic structure of graphene tubules based on C60,” *Physical Review B*, vol. 46, no. 3, (1992) 1804–1811.

[9] J.-C. Charlier, X. Blase, and S. Roche, “Electronic and transport properties of nanotubes,” *Reviews of Modern Physics*, vol. 79, no. 2. *American Physical Society* (APS), pp. 677–732, May 16, 2007.

[10] G. Dresselhaus, M. S. Dresselhaus, and P. C. Eklund, *Science of Fullerenes and Carbon Nanotubes*, Academic Press, San Diego, Calif, USA, 1996.

[11] J. Sha et al., “Silicon Nanotubes,” *Advanced Materials*, vol. 14, no. 17. *Wiley*, pp. 1219–1221, Sep. 03, 2002.

[12] M. Nath, A. Govindaraj, and C. N. R. Rao, “Simple Synthesis of MoS2 and WS2 Nanotubes,” *Advanced Materials*, vol. 13, no. 4. *Wiley*, pp. 283–286, Feb. 2001.
.

[13] U. K. Gautam, S. R. C. Vivekchand, A. Govindaraj, G. U. Kulkarni, N. R. Selvi, and C. N. R. Rao, “Generation of Onions and Nanotubes of GaS and GaSe through Laser and Thermally Induced Exfoliation,” *Journal of the American Chemical Society,* vol. 127, no. 11. American Chemical Society (ACS), pp. 3658–3659, Feb. 24, 2005.

[14] A. Naderi, S. M. Noorbakhsh, and H. Elahipanah, “Temperature Dependence of Electrical Characteristics of Carbon Nanotube Field-Effect Transistors: A Quantum Simulation Study*,” Journal of Nanomaterials*, vol. 2012. *Hindawi Limited*, pp. 1–7, 2012. doi: 10.1155/2012/532625.

[15] J. Deng and H.-S. P. Wong, “A compact SPICE model for carbon-Nanotube field-effect transistors including nonidealities and its application—Part II: Full device model and circuit performance benchmarking,” *IEEE Trans. Electron Device*, vol. 54, no. 12, (2007) 3195–3205.

[16] C. J. Cramer, “Essentials of Computational Chemistry”, John Wiley & Sons, Inc., USA, 2002.

[17] D. K. Singh,"Tight Binding Modeling of Two Dimensional and Quasi –Two Dimensional materials”, Bilkent University, (2017) 71.

[18] D. Dass, R. Vaid, "Chirality dependence of electronic band structure and density of states in singlewalled carbon nanotubes", *The African Review of Physics* ,vol. 12, (2017) 104 – 113.

[19] D. Dass, R. Prasher and R.Vaid, "Analytical Study of Unit Cell and Molecular Structures of Single Walled Carbon Nanotubes", *International Journal Of Computational Engineering Research*, Vol. 2 Issue. 5, (2012)1447-1457.

[20] S. Mishra1 and R.P. Agarwal2, "Band Structure and Density of States Computational Analysis of mSWCNT for different Structural Parameters*", International Journal of Advanced Research,* Vol. 3, no.7, (2015) 684-690.

[21] D. S. Hien, N. T. Luong, T. T. A. Tuan, and D. V. Nga, “Modeling of planar carbon nanotube field effect transistor and three-dimensional simulation of current-voltage characteristics,” *Journal of Physics: Conference Series*, vol. 187. *IOP Publishing*, p. 012049, Sep. 01, 2009

[22] R. Nizam and M. Sehban: "Calculating the Band Gaps of Perfect Carbon Nanotube through Tight Binding Method". *International Journal of Science and Research* (*IJSR*), vol. 6,(2017) 1565-1570.

[23] J. K. Fodor: "Simulation involving carbon nanotubes and nanoribons”. Thesis, University of Florida, (2007) 94.

[24] J.-P. . Issi, L. Langer, J. Heremans, and C. H. Olk, “Electronic properties of carbon nanotubes: Experimental results,” *Carbon*, vol. 33, no. 7, pp. 941–948, 1995, doi: https://doi.org/10.1016/0008-6223(95)00023-7.

[25] J. Appenzeller, J. Knoch, M. Radosavljević, and Ph. Avouris, “Multimode Transport in Schottky-Barrier Carbon-Nanotube Field-Effect Transistors,” *Physical Review Letters*, vol. 92, no. 22. *American Physical Society (APS),* Jun. 04, 2004. doi: 10.1103/physrevlett.92.226802.

[26] M. Tiwari, K. K. Sharma, L. S. Rawat and V. C. Kohli: "Impact of Oxide Thickness on Gate Capacitance, Drain Current and Transconductance A Comprehensive Analysis on MOSFET, Nanowire FET and CNTFET Devices". *International Journal for research in emerging science and techonology*, vol. 2, (2015) 73 -85.